

Nanoscale

Accepted Manuscript



This is an *Accepted Manuscript*, which has been through the Royal Society of Chemistry peer review process and has been accepted for publication.

Accepted Manuscripts are published online shortly after acceptance, before technical editing, formatting and proof reading. Using this free service, authors can make their results available to the community, in citable form, before we publish the edited article. We will replace this *Accepted Manuscript* with the edited and formatted *Advance Article* as soon as it is available.

You can find more information about *Accepted Manuscripts* in the [Information for Authors](#).

Please note that technical editing may introduce minor changes to the text and/or graphics, which may alter content. The journal's standard [Terms & Conditions](#) and the [Ethical guidelines](#) still apply. In no event shall the Royal Society of Chemistry be held responsible for any errors or omissions in this *Accepted Manuscript* or any consequences arising from the use of any information it contains.

Journal Name

ARTICLE

Unusual Role of Folate in the Self-Assembly of Heparin-Folate Conjugates into Nanoparticles

Jianquan Wang,^a Daoshuang Ma,^a and Qian Lu,^a Shaoxiong Wu,^b Gee Young Lee,^c Lucas A. Lane,^c Bin Li,^a Li Quan,^a Yiqing Wang,^{*a,c} Shuming Nie^{*a,c}

Received 00th January 20xx,
Accepted 00th January 20xx

DOI: 10.1039/x0xx00000x

www.rsc.org/

Tumor targeting agents including antibodies, peptides, and small molecules, are often used to improve the delivery efficiency of nanoparticles. Despite the numerous studies investigating the abilities of targeting agents increasing accumulation of nanosized therapeutics within diseased tissues, little attention has focused on how these ligands can affect the self-assembly of the nanoparticle's modified polymer constituents upon chemical conjugation. Here we present an actively tumor targeted nanoparticle constructed via self-assembly of folate modified heparin. Folate conjugation unexpectedly allowed the self-assembly of heparin, where a majority of the folate molecules (>80%) resided inside the core of the nanoparticle. The folate-heparin nanoparticles could also physically encapsulate lipophilic fluorescent dyes, enabling the use of the constructs as activatable fluorescent probes for targeted *in vivo* tumor imaging.

Introduction

Numerous constructions of self-assembled polymer nanoparticles have been developed for the delivery of therapeutic and imaging agents.¹⁻² When targeting cancerous tumors, nanoparticles can utilize the enhanced permeation and retention (EPR) effect and chemically active ligands to increase accumulation of injected doses within diseased areas.³⁻⁴ Passive targeting takes advantage of the EPR effect which depends on the size of nanoparticles and the unique properties of leaky tumor vasculature.^{4,5-6} Active targeting, in addition to the EPR effect, will use tumor specific ligands including antibodies, peptides, and small molecules, to help maintain nanoparticle concentrations within the tumor.^{4,7} Studies on active targeting typically focus on demonstrating the improved tumor retention or uptake of nanoparticles,⁸⁻¹¹ yet less attention has been placed on how chemically conjugated moieties can affect the self-assembling process of the modified polymers which constitute the nanoparticle.

Naturally occurring folic acid (folate) has several advantages as an active tumor targeting agent such as having facile conjugation chemistry, while exhibiting lower immunogenicity and cost than antibodies.¹²⁻¹³ Since the folate receptor (FR) is over-expressed in many types of solid tumors (e.g. ovarian, uterine, lung, breast, and head and neck) folate is widely useful as an active targeting agent for a variety of cancers.¹⁴⁻¹⁵ A number of folate modified

nanoparticles reported are shown to have excellent specific binding properties *in vitro* and *in vivo*.¹⁶⁻¹⁷ Recently, the Langer group discovered that not all of the folate are displayed on the surface of nanoparticles self-assembled from folate-PEG-PLGA polymers.¹⁸ The authors suspected that the unusual outcome of folate mostly residing within the nanoparticle core, rather than at the outer surface, was due to the lower solubility of the molecule compared to the polymer. However, these conclusions were derived from indirect evidence of lower cellular binding than what was expected.

In this study we further explore the effects of folate molecules on the self-assembly of folate-polymer conjugates into nanoparticles. Here we use a simple model system of folate-heparin conjugates which can self-assemble into nanoparticles of 40 ± 15 nm with high monodispersity (polydispersity < 0.2). We demonstrate NMR methods which provide direct evidence of the nanoparticles to have 15-18% of the folate ends of the conjugates directed towards the surface of the nanoparticles with the rest buried within the core. These methods also identified that the mechanism behind the conjugated folates' ability to self-assemble water soluble polymers into nanoparticles is via hydrogen bonding networks and hydrophobic interactions between folate groups of the conjugate polymers inducing a liquid crystalline state within the nanoparticle core. Realizing this property, we used folate-heparin nanoparticles to encapsulate lipophilic dyes and demonstrate their utility as activatable probes for *in vivo* tumor imaging.

Experimental

Materials

Heparin (sodium salt form, average Mw:13,000) was purchased from Celsus Laboratories (Cincinnati, OH). Fluorescent lipophilic dye DiIC₁₈(5) (1,1'-dioctadecyl -3,3',3'-tetramethylindodicarbocyanine, 4-chlorobenzenesulfonate salt) was obtained from Invitrogen. Milli-Q deionized (DI) water (Millipore, $18.2 \text{ M}\Omega \text{ cm}^{-1}$) was used

^a Department of Biomedical Engineering, College of Engineering and Applied Sciences, Nanjing University, Nanjing, Jiangsu Province 210093, China.

^b Department of Chemistry, Emory University, Atlanta, Georgia 30322, USA

^c Department of Biomedical Engineering, Emory University and Georgia Institute of Technology, Atlanta, Georgia 30322, USA

Email: wangyiqing@nju.edu.cn; snie@emory.edu

Electronic Supplementary Information (ESI) available: [NMR spectra and fluorescent images of HF-488 with cancer cells are included]. See DOI: 10.1039/x0xx00000x

throughout the experiments. Anhydrous methylsulfoxide (DMSO) and N, N-dimethylformamide (DMF) were obtained from EMD chemicals (France). Dialysis membrane Spectra/Por 3 (MWCO: 3,500) was purchased from Spectrum Labs. All other reagents were obtained from Sigma-Aldrich (St Louis, MO) at highest purity available.

Instrumentation

The surface charge (zeta potential) and size of the folate-heparin nanoparticles were measured by the ZetaSizer Nano-ZS90 (Malvern Instrument). Absorption spectra were obtained by an ultraviolet-visible spectrophotometer (Beijing Persee DU1900). Fluorescent spectra were obtained by a Fluoromax-2 (Jobin Yvon-Spex, Horiba Group). NMR spectra were obtained from either an INOVA 600 or INOVA 400. *In vivo* fluorescent images of mice specimens were taken by a Kodak Imaging Station IS4000MM using a 625 nm band pass excitation filter and a 700 nm long pass emission filter.

Synthesis of Heparin-Folate Polymer Conjugates

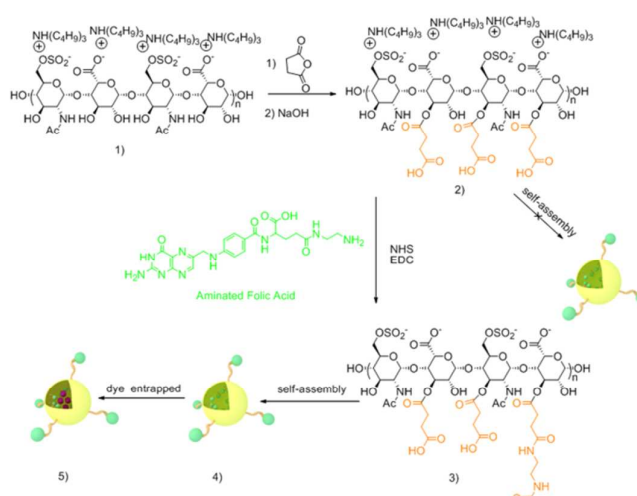
Succinic anhydride modified heparin (H-Su, 0.200 g, prepared according to a previously reported procedure¹⁹) was dissolved in DI water (10 mL), and of the solution was adjusted to 6.0 pH by tributylamine. The resulting solution was lyophilized at -50 °C resulting in a H-Su tributylammonium salt (0.400 g). The H-Su tributylammonium salt (0.400 g) was dissolved in anhydrous DMSO (10 mL) together with NH₂-modified folic acid (0.082 g, 0.17 mmol, prepared according to previously reported procedure¹⁴), EDAC (0.065 g, 0.34 mmol) and NHS (0.024 g, 0.21 mmol), and the reaction was allowed to proceed at 35 °C for 24 h. The reaction mixture was dialyzed against DI water for 24 h to remove the solvent and catalysts (Spectra/Por 3, MWCO: 3,500), and the resulting solution was concentrated and passed through an ion exchange column (Dowex-50, H⁺ form, 200 mL). The collected solution was adjusted to 7 pH by NaOH aqueous solution (0.10 M) followed by dialysis in DI water again for 24 h. After lyophilization, heparin-folate (0.220 g) was obtained as a yellow powder. ¹H NMR (D₂O): δ 1.9-2.0 ppm (-NHCOCH₃, succinylated-heparin), 2.4-2.8 ppm (-CH₂CH₂-CONH-, succinylated-heparin), 3.2-3.6 ppm (heparin), 4.4-5.8 ppm (heparin). 6.6 ppm (folate), 7.7 ppm (folate), 8.6 ppm (folate).

Critical Micelle Concentration (CMC) Measurement

The CMC of HF nanoparticle was determined by the reported procedure.²⁰

Preparation of Heparin-Folate (HF) and Heparin-Folate-DiIc₁₈(5) (HF-DiI) Nanoparticles

The heparin-folate conjugate (100 mg) either with or without the addition of the dye DiIc₁₈(5) (2 mg) was dissolved in DMSO (5 mL). The mixture was dialyzed against DI water for 24 h (Spectra/Por6, MWCO: 8000), followed by lyophilization. The resulting yellow (no dye, HF) or light blue power (with dye, HF-DiI) was re-suspended in PBS under gentle shaking. (Scheme 1)



Scheme 1 Preparation and characterization of activatable HF-DiI fluorescent nanopores. 1) Structure of heparin-tributylamine salt; 2) Structure of succinylated heparin; 3) Structure of HF polymer; 4) HF Polymer self-assembling into NPs; 5) Polymer and dye self-assembling into NPs, resulting in dye aggregates which self-quench their fluorescence.

Determination of the Ratio between Folate at the Surface and Inside the Core of HF Nanoparticle by NMR

The ratio between folate on the surface and folate inside the core of HF nanoparticle was determined by the following two methods:

Method 1. The total content of folate conjugated on to the HF NP which was estimated comparing UV absorption intensity at 360 nm of the DMSO solution of heparin-folate vs a standard curve, which was generated by a series of known concentrations of folic acid solutions in DMSO. The percentage of the folate on HF surface was quantified by ¹H NMR: HF (10.00 mg) and pyridine (0.200 mg, as internal reference) in D₂O (0.60 mL). The amount of folate on the surface can be estimated by comparing the integration value between the folate and pyridine peaks within the spectrum of the sample. The percentage of the folate on the NP surface were calculated by the following equation:

$$(\text{folate on the surface})\% = (\text{surface folate concentration determined by NMR}) / (\text{total folate concentration determined by UV-Vis})$$

Method 2. Two HF samples in the different solvents were prepared: A. HF (10.00 mg) in D₂O (0.60 mL) and B. HF (10.00 mg) in D₂O/*d*-DMSO mixture (D₂O:*d*-DMSO = 1:3 v/v, 0.15 mL D₂O, 0.45 mL *d*-DMSO). The samples were added into NMR tubes (OD=5 mm) with a coaxial insert, in which *d*-Chloroform (120 μL, containing CHCl₃ 0.2% in volume) was loaded. The total amount of folate conjugated onto HF was estimated by comparing the integration value between the folate and CHCl₃ in D₂O/*d*-DMSO mixture, and the folate on the surface was estimated by comparing the integration value between the folate and CHCl₃ in D₂O.

Cell Culture

Human epidermoid carcinoma cell line KB-3-1 and epithelial lung carcinoma cell line A549 were obtained from ATCC (Manassas, VA, USA). Cells were maintained in RPMI 1640 culture media

supplemented with 10% heat-inactivated fetal bovine serum (FBS) and antibiotics in a 37 °C, 5% CO₂ humidified incubator.

Cellular uptake of HF by KB-3-1 and A549 cells

Fluorescent dye Oregon Green 488-labeled HF nanoparticles (HF-488) were prepared from reacting amine functionalized Oregon green 488 cadaverine (Invitrogen) and HF in DMSO at room temperature overnight, followed by dialysis against water (Spectra/Por 6, MWCO:8000). The unreacted Oregon green 488 dye was removed by PD-10 column. KB-3-1 or A549 cells were incubated with HF-488 NPs (4 µg/mL of Oregon Green 488 concentration) for four hours at 37 °C, and then washed for two hours at 37 °C, and then washed three times with PBS and analyzed by flow cytometry.

In Vivo Imaging

Nude mice (athymic nu/nu, Taconic, NY), aged 4 to 6 weeks (about 20 g weight) were used for in vivo imaging. KB-3-1 cells (1×10^6 cells per mouse) were injected subcutaneously into the right flank of male nude mice. Direct injection of the NPs under the skin of the same mouse was used for comparison. All animal experiments were performed in accordance with the laws and regulations of Emory University, and approved by the Animal Care and Use Committee of Emory University.

Results and discussion

Folate Induces the Self-assembly of HF

Several groups have reported folate's ability to self-assemble into liquid crystalline phases through Hoogsteen-type hydrogen bonding in the aqueous media,²¹ however, to our knowledge, no one has reported how folate conjugation can induce the self-assembly of hydrophilic polymers into a nanoparticle. We found that H-Su was completely soluble in DI water at neutral pH, and no nanoparticle formation could be detected by DLS measurements, but once folate was chemically conjugated onto the H-Su polymers, monodisperse HF nanoparticles formed in water spontaneously. In addition to DLS, we also confirmed nanoparticle formation by imaging samples through scanning electron microscopy (SEM) (Fig.1). The CMC of HF nanoparticle was 2×10^{-3} mg/mL.

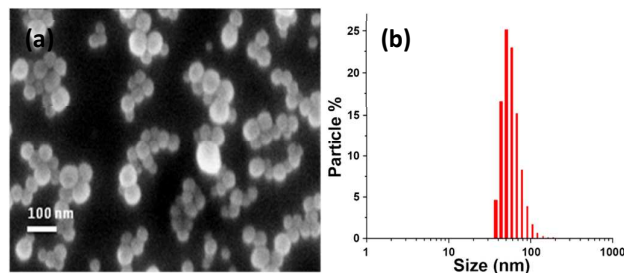


Fig.1 (a) SEM image of HF NPs; and diameter = 35 ± 10 nm), (b) DLS measure of HF-Dil NPs (hydrodynamic diameter = 40 ± 15 nm)

In contrast to other reports on heparin-based NPs bearing hydrophobic moieties such as deoxycholic acids or taxol,⁷ interestingly our HF nanoparticles modified with succinic anhydride

and folic acid were presumed not hydrophobic enough to promote self-assembly. We examined the water solubility of H-Su which resulted in 100 mg/mL at 25 °C, while the water solubility of free folic acid is about 1.6×10^{-3} mg/mL. We hypothesize that the driving force for the unusual self-assembly of HF is a result from combined interaction of FA-succinic acid hydrogen bonding, weak hydrophobicity from three -CH₂- groups of succinic acid and low water solubility of folate. Since the folate grafts can accumulate throughout the polymer, the micelles will form via a mixture of middle or distal polymer ends within the core or on the outer surface. Randomization of hydrophobic grafts on longer hydrophilic backbones in co-block polymer systems have been previously shown to have smaller micelle sizes than those with end-directed grafting due to such an assembly process.²² The regions of HF polymers containing dense populations of folate will be directed towards the core of the micelles, whereas regions displaying one to a couple of folates can remain on the outside of the micelle as their local hydrophobicity is not enough to outweigh the favorable solvation interactions and configurational entropy of the heparin subunits in water.

Determining the Ratio between folate on the surface and Inside the Core of HF Nanoparticles by ¹H NMR

We demonstrate that once HF self-assembles, folate inside the nanoparticle cannot be solvated by water, and we can consider that it is in the liquid crystalline phase. Using conventional liquid-state ¹H NMR for analysis of the HF nanoparticle samples, we find that the peaks of folate molecules within the core contributing to the spectra are flat and broad due to strong dipolar coupling resulting from a condensed state. Folate molecules residing on the surface of the nanoparticles, on the other hand, are well solvated by water, and therefore have spectral peaks which are sharp and narrow because dipolar couplings average to zero for the fast molecular motions of solvated molecules. Thus integration of the sharp spectral peaks of folate molecules determines the concentration of molecules which are solvated and residing on the surface of the nanoparticles and excludes the folates buried within the condensed phase of the core. (Fig.2)

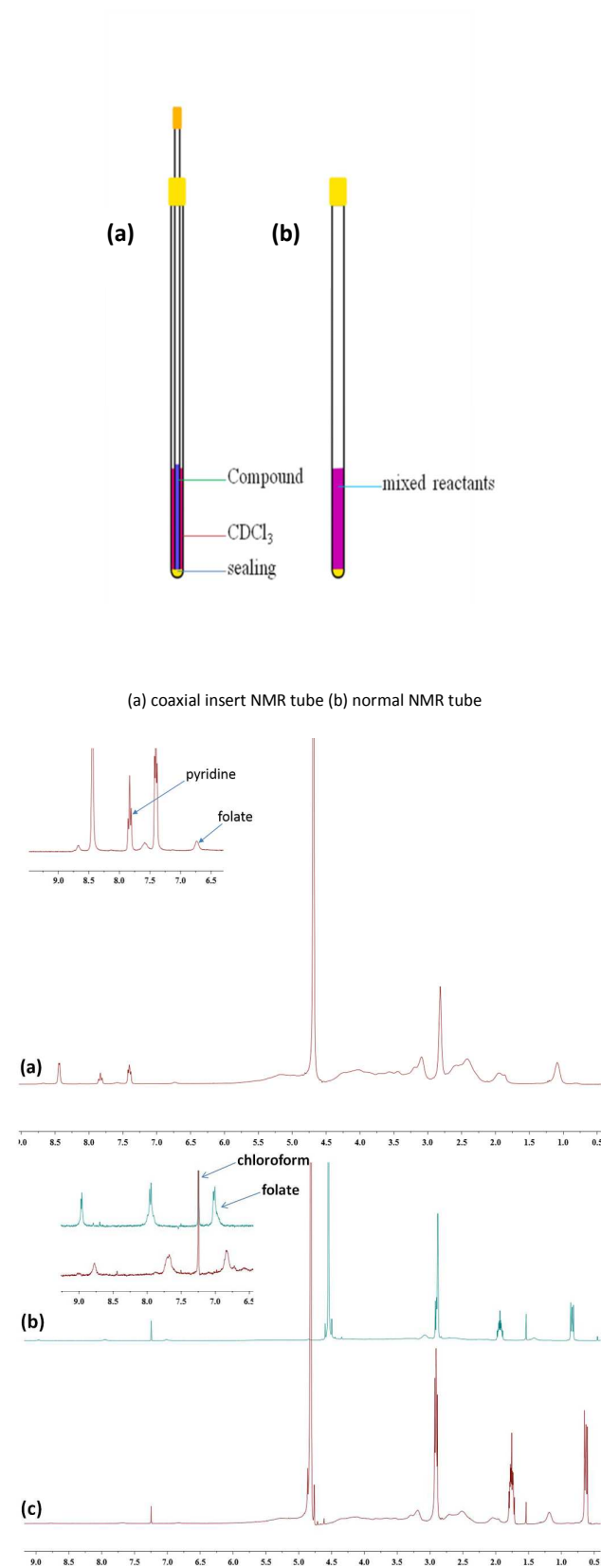


Fig. 2 ¹H NMR spectra for the weight percentage of the folate on the NP surface with different method; (a) HF NP (10 mg) in D₂O with pyridine(0.2 mg) as the internal standard ;(b) HF NP (2.5 mg/mL) in the presence of *d*-Chloroform (99.8%)

in *d*-DMSO/D₂O (v/v, 3:1); (c) HF NP (10 mg/mL) in the presence of *d*-Chloroform (99.8%) in D₂O.

To determine whether all the conjugated folate moieties participate the self-assembly of HF, we design two methods:

Method 1. Folate has two characteristic UV absorption peaks at 280 nm and 360 nm, while H-Su has no UV absorption within this range. Therefore, we can determine the total folate content by comparing the UV absorption intensity of the HF DMSO solution (0.825 mg/mL, no nanoparticles formation observed at this concentration) to the calibration curve generated by a series of folic acid DMSO solutions with known concentrations. We estimated that the total folate is 11.83 wt% of the HF nanoparticle, which is about 3 folate molecules/heparin chain (based on heparin average molecular weight \sim 13,000). To quantify the folate on the surface, we prepared HF samples in D₂O (10.0 mg HF in 0.6 mL D₂O, of which folate is about 1.183 mg) with added pyridine (0.200 mg) as an internal reference. Pyridine proton signals are δ 7.4, 7.8, and 8.4 ppm, while folate phenyl proton signals are 6.6, 7.7, 8.6 ppm. By comparing the integration values of folate at 6.6 ppm with pyridine at 7.8 ppm, we estimated the solvated folate of the sample to be 0.179 mg. From the UV measurements, the total folate amount within the sample was determined to be 1.183 mg. Therefore, the ratio between folate on the surface of HF nanoparticle to the total folate is 15.1%.

Method 2. Since the addition of pyridine as the internal reference for Method 1 may potentially interfere the self-assembly of HF, we developed a 2nd method in which HF samples were loaded in a NMR tube equipped with a coaxial insert containing *d*-Chloroform as the internal reference. Here, the HF solution in the center of the tube is walled off and surrounded by a solution of *d*-Chloroform. The chloroform proton signals at 7.27 ppm do not overlap with the folate phenyl peaks.

We prepared HF samples in D₂O and in a mixture of D₂O/*d*-DMSO (1:3 v/v). When D₂O was used as the solvent, HF self-assembled into nanoparticles where only the folate molecules on the surface of nanoparticles could be measured; while when a D₂O/*d*-DMSO solvent mixture was used, the HF nanoparticles disassembled, allowing all the folate conjugated onto the H-Su polymers to be measured. To account for variations in NMR experimental parameters, such as lock power and gain power, we used chloroform as an internal reference. In both experiments, we set the chloroform peak area to 1. Since the concentration of chloroform remains constant between both experiments, we can estimate the increase of folate phenyl peak areas from disassembled samples in the D₂O/*d*-DMSO solvent mixture from the assembled samples in D₂O. From this analysis we determined the surface folate to be 18.1% of the total folate of the nanoparticles, which is in consistent with the first method. (See SI for the detailed procedure)

Active Targeting Effects not Compromised

KB-3-1 (FR positive) and A549 (FR negative) cells were incubated with HF-488 NPs (4 μ g/mL of dye concentration) with or without 1 mmol/L free folate for four hours at 37 $^{\circ}$ C, and then washed three times with PBS and analyzed by flow cytometry. The results showed that HF uptaken by KB-3-1 is 4 times as much by A549. (Table 1).

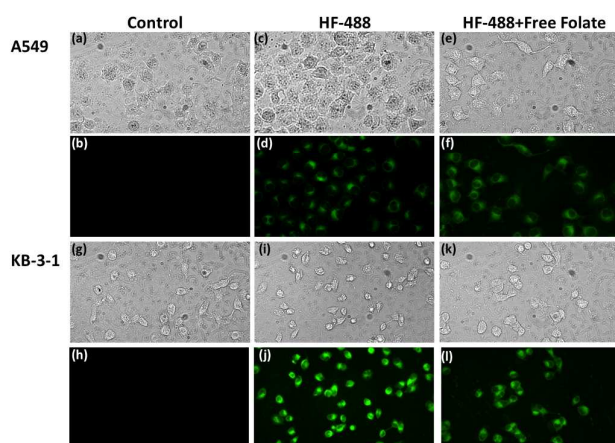


Fig. 3 Fluorescent images of KB-3-1 and A549 cells incubated with HF-488 NPs for 4h (a, c, e, g, i, k: bright field; b, d, f, h, j, l: Fluorescent images 500 \times).

Sample	Mean Fluorescence	
	KB-3-1	A549
Control	5.34	7.64
HF-488	91.24	22.90
HF-488+Free Folate	47.73	21.06

Table 1. Cellular uptaken of HF-488 NPs by KB-3-1 (folate receptor overexpressed cell lines) and A549 (folate receptor deficient cell lines)

Activatable fluorescent nanoprobe nanoparticle

Since the folates within the interior of the nanoparticles are thought to act like a condensed hydrophobic phase, we questioned whether such an interior can be exploited for the use of carrying lipophilic molecules such as organic fluorophores and/or therapeutics. To test whether the HF particles had the ability to act as carriers for hydrophobic molecules, we used the NIR dye DiI_{C18}(5) as a model. DiI_{C18}(5) is a near-infrared (NIR) lipophilic fluorescent dye which has an emission maximum peak around 670 nm in methanol. The low water solubility and low toxicity make DiI an ideal candidate to prepare fluorescent nanoprobes. The weight percentage of DiI entrapped by the HF NPs (about 1%) which was determined by comparing UV absorption intensity of a diluted DMSO solution of HF-DiI NPs against a standard curve generated by a solution series of known DiI concentrations in DMSO. The concentration of entrapped DiI was extremely high inside HF-DiI NPs, which led to fluorescence self-quenching of DiI. As a result, NPs in the assembled state have weak fluorescence. These weakly fluorescent nanoprobes can be activated by adding DMSO, which dissociates HF-DiI NPs to release free DiI. Compared with emission spectra of HF-DiI in water and DMSO, a 60 fold fluorescence increase in DMSO was observed (Fig.4) along with a 10 nm blue shift of fluorescent emission maximum peak position, which is a typical indication of deaggregation of dye molecules.

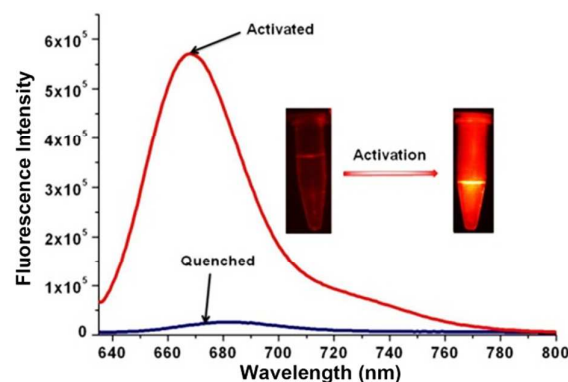


Fig.4 Fluorescent spectra and fluorescent images of HF-DiI NPs with same concentration in DMSO and water.

In vivo tumor imaging

To demonstrate the nanoprobes could be activated *in vivo*, HF-DiI NPs were directly injected into subcutaneous KB-3-1 tumor xenografts within a mouse model; direct injection of the NPs under the skin of the same mouse was used for comparison. No fluorescent signals of DiI were detected from both injections sites after 1 h. 2 h after injection, the tumor started to become fluorescent while it took another 2 h for skin spot started to show DiI signals. When cells uptake these nanoparticles they are in harsh acidic and enzymatic environments of the late endosomes lysosomes which most likely cleave bonds such as esters and dissemble nanoparticles. Cells with more receptors usually have faster uptake of particles⁴ and would presume to activate the fluorescence at quicker rates. After 24 h, the fluorescent intensities of both sites became more than 5 times brighter than surrounding areas (Fig.5).

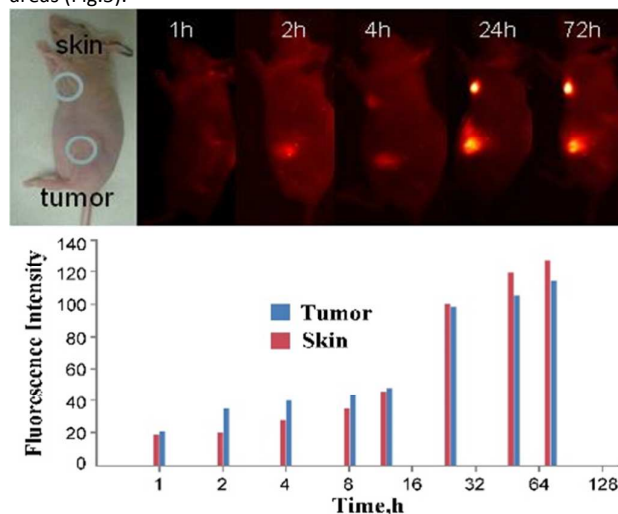


Fig.5 Top: direct injection of HF-DiI (0.5 mg NP/mL in PBS, DiI content = 1.2% w/w, 10 μ L) into tumor and under skin. Images were taken by Kodak Image Station with a 625 nm excitation filter and a 700 nm emission filter at 1, 2, 4, 24, and 72h; Bottom: Fluorescence intensity changes over 72 h at injected spots.

Conclusions

In conclusion, we studied the unexpected self-assembly of folate modified heparin nanoparticles. We demonstrated two simple methods which allowed us to directly determine the number of heparin-folate molecules which displayed the folate ends towards the surface of the nanoparticles. We found that only 15-18% of total conjugated folate was on the surface, while the rest was inside the core due to imparting a hydrophobic segment to hydrophilic heparin polymers enabling self-assembly of the conjugates into nanoparticles. Furthermore, we discovered that the folate was not only able to promote the self-assembly of folate-heparin, but also enable the nanoparticles to physically encapsulate lipophilic fluorescent dyes, which allow the nanoparticles use as an activatable fluorescent probe for *in vivo* tumor imaging.

Acknowledgements

This work was supported by grants from the NCI Centers of Cancer Nanotechnology Excellence (CCNE) Program (U54CA119338) and the Start-up fund from Nanjing University. Prof. Yiqing Wang gratefully acknowledges "Jiangsu Specially -Appointed Professor" award.

Notes and references

1. F. Alexis, E. M. Pridgen, R. Langer and O. C. Farokhzad, *Handb Exp Pharmacol*, 2010, 55-86.
2. S. K. Sahoo and V. Labhasetwar, *Drug Discov Today*, 2003, **8**, 1112-1120.
3. K. Cho, X. Wang, S. Nie, Z. G. Chen and D. M. Shin, *Clin Cancer Res*, 2008, **14**, 1310-1316.
4. L. A. Lane, X. Qian, A. M. Smith and S. Nie, *Annu. Rev. Phys. Chem.*, 2014.
5. Y. Matsumura and H. Maeda, *Cancer Res*, 1986, **46**, 6387- 6392.
6. S. K. Hobbs, W. L. Monsky, F. Yuan, W. Gregory Roberts, L. Griffith, V. P. Torchilin and R. K. Jain, *Medical Sciences*, 1998, **95**, 4607-4612.
7. T. M. Allen, *Nat rev. Cancer*, 2002, **2**, 750-763.
8. C. H. J. Choi, C. A. Alabi, P. Webster and M. E. Davis, *Proc. Nat. Acad. Sci.*, 2010, **107**, 1235-1240.
9. X. Huang, X. Peng, Y. Wang, Y. Wang, D. M. Shin, M. A. El-Saye and S. Nie, *ACS Nano*, 2010, **4**, 5887-5896.
10. U. S. Dinish, G. Balasundaram, Y.-T. Chang and M. Olivo, *Sci. Rep.*, 2014, **4**.
11. X. Qian, X.-H. Peng, D. O. Ansari, Q. Yin-Goen, G. Z. Chen, D. M. Shin, L. Yang, A. N. Young, M. D. Wang and S. Nie, *Nat. Biotechnol.*, 2007, **26**, 83-90.
12. W. Xia and P. S. Low, *J Med Chem*, 2010, **53**, 6811-6824.
13. P. S. Low and S. A. Kularatne, *Curr Opin Chem Biol*, 2009, **13**, 256-262.
14. X. Wang, J. Li, Y. Wang, K. J. Cho, G. Kim, A. Gjyzezi, L. Koenig, P. Giannakakou, H. J. C. Shin, M. Tighiouart, S. Nie, Z. Chen and D. M. Shin, *ACS Nano*, 2009, **3**, 3165-3174.
15. S. Iwakiri, M. Sonobe, S. Nagai, T. Hirata, H. Wada and R. Miyahara, *Ann Surg Oncol*, 2008, **15**, 889-899.
16. C. P. Leamon and J. A. Reddy, *Adv drug delivery rev*, 2004, **56**, 1127-1141.
17. C. Yue, P. Liu, M. Zheng, P. Zhao, Y. Wang, Y. Ma and L. Cai, *Biomaterials*, 2013, **34**, 6853-6861.
18. P. M. Valencia, M. H. Hanewich-Hollatz, W. Gao, F. Karim, R. Langer, R. Karnik and O. C. Farokhzad, *Biomaterials*, 2011, **32**, 6226-6233.
19. Y. Wang, Y. Wang, J. Xiang and K. Yao, *Biomacromolecules*, 2010, **11**, 3531-3538.
20. G. Kwon, M. Naito, M. Yokoyama, T. Okano, Y. Sakurai and K. Kataoka, *Langmuir*, 1993, **9**, 945-949.
21. F. Ciuchi, G. Di Nicola, H. Franz, G. Gottarelli, P. Mariani, M. G. Ponzi Bossi and G. P. Spada, *J. Am. Chem. Soc*, 1994, **116**, 7064-7071.
22. F. M. Winnik, A. R. Davidson, G. K. Hamer and H. Kitano, *Macromolecules*, 1992, **25**, 1876-1880.